Mechanism of toxic action of cationic G5 and G7 PAMAM dendrimers in the cyanobacterium *Anabaena* sp. PCC 7120

Cyanobacterial physiology impaired by high generation dendrimers

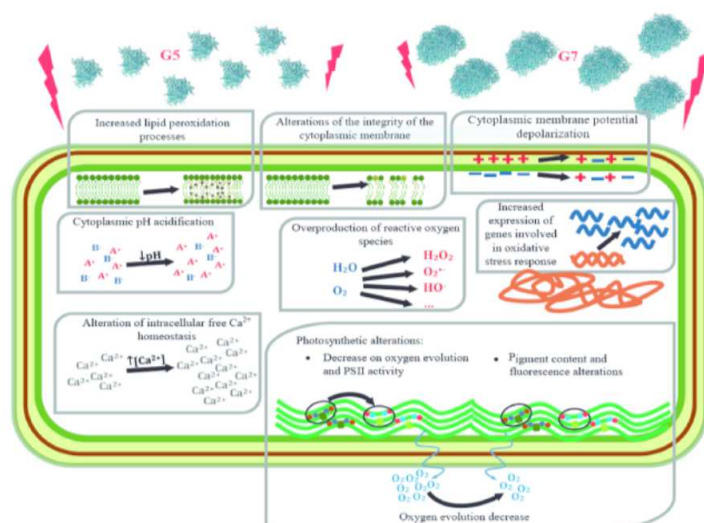# Mechanism of toxic action of cationic G5 and G7 PAMAM dendrimers in the cyanobacterium *Anabaena* sp. PCC 7120

Miguel Tamayo-Belda[a], Miguel González-Pleiter[a], Gerardo Pulido-Reyes[a], Keila Martin-Betancor[a], Francisco Leganés[a], Roberto Rosal[b], Francisca Fernández-Piñas[a,*]

[a] Department of Biology, Universidad Autónoma de Madrid, 28049 Madrid, Spain.
[b] Department of Chemical Engineering, Universidad de Alcalá, E-28871, Alcalá de Henares, Madrid, Spain.

* Corresponding author: francisca.pina@uam.es

Abstract

Nowadays, nanomaterials are extensively used worldwide in many different fields and their potentially serious effects in aquatic ecosystems have become a global concern. In this study, we have investigated the effect of two nanometric manufactured polymers, high-generation cationic G5 and G7 poly(amidoamine) dendrimers, in a prokaryotic primary producer of aquatic ecosystems, the filamentous cyanobacterium *Anabaena* sp. PCC7120. Dendrimers significantly decreased the growth of the cyanobacterium and they induced morphological alterations both at the filaments and single cell level. Furthermore, the exposure to dendrimers induced significant alteration in several physiological parameters of the cyanobacterium: intracellular reactive oxygen species overproduction, damage in membrane integrity, membrane potential alterations, increase of metabolic activity, acidification of intracellular pH, oxidative DNA damage and alteration of intracellular free Ca^{2+} homeostasis. Dendrimers also induced alterations in the photosynthesis of *Anabaena*: decrease in oxygen evolution and in PSII activity, alteration in different photochemical events and in chlorophyll *a* content. Moreover, both dendrimers were internalized into cyanobacterial cells. In conclusion, high-generation cationic dendrimers exhibited high toxicity towards *Anabaena* severely affecting several physiological, morphological, and photosynthetic parameters.

Introduction

Dendrimers are a type of hyperbranched nanometric polymers synthetized in an iterative sequence that allows them to present a radially symmetric shape with well-defined, homogeneous, and monodisperse structure, distinguishing an inner and an outer shell; one of the most common is based on poly(amidoamine), noted as PAMAM dendrimer[1]. The consecutive repetition of iterations increases the radius in a controlled way producing spherical hyperbranched topology radiating from a central core and growing generation by generation[2,3]. This structure presents large number of surface end-groups susceptible to react with other molecules and shows internal cavities which may serve to encapsulate active chemical compounds, reason whereby dendrimers have been developed as drugs carriers in biomedicine, one of their main application fields[4,5].

The rapid development of nanoscience with advances in essential areas such as agriculture, industry, energy or biomedicine is a cause for concern due to the possible dissemination of emerging pollutants in the environment, whereby ecotoxicological research must consider them in order to reach an adequate regulation framework[6–8]. Currently, both low and high generations dendrimers are being developed not only as drugs carriers in biomedicine[5,9–11], but also in water treatment for heavy metals removal[12–14], in catalysis engineering[15], as well as in the development of metal ion sensors[16]. In this context and given the wide range of potential applications, the OECD has included PAMAM dendrimers in the list of nanoparticles to be screened for possible toxicological effects in both environmental and mammalian systems[17].

In spite of the increased development of dendrimer-based materials, there is a lack of information on their potential ecotoxicological effects[18], in particular regarding the monitoring of biological effects of higher generation dendrimers. Nevertheless, regarding the potential human health effects, PAMAM toxicity dendrimers have been evaluated in different organisms as a function of their generation (size), dose, exposure time, core and surface functionalization[19–24]. However, there are few studies in the literature concerning the toxicity of PAMAM dendrimers on organisms of environmental relevance[22,25–31].

Cyanobacteria are a unique group among prokaryotes capable to perform oxygenic photosynthesis; some of them are also able to use atmospheric nitrogen. Cyanobacteria have also generated symbiotic relationships with diatoms, sponges, corals, lichens, ferns, as well as mutalistic associations with different organisms spreading their potential habitats and improving nutrient availability[32]. As primary producers, any toxic effect on them, may seriously affect the aquatic trophic chain. The filamentous

cyanobacterium *Anabaena* sp. PCC7120 (hereinafter, *Anabaena*) was selected as a model organism, given its environmental relevance and ubiquity, as well as the extensive bibliography regarding the genetic, physiology and ecological importance. Furthermore, this cyanobacterium has been used regularly as model for ecotoxicological studies, including the field of nanotoxicology[31,33–40].

In this work, high generation PAMAM dendrimers have been tested towards the filamentous cyanobacterium *Anabaena* to study their toxic mode of action. Toxic effects of cationic G5 and G7 PAMAM dendrimers were analyzed taking into account growth inhibition, cyanobacterium morphology (cell shape, filament length, internal complexity and ultrastructure), physiological endpoints (membrane integrity, membrane potential, intracellular pH, intracellular free calcium, disbalance in reactive oxygen species (ROS) production, lipid peroxidation and metabolic activity), gene expression studies (transcription level of three genes involved in the response to oxidative stress) and photosynthetic related parameters (oxygen evolution, PSII activity, pigment content and their *in vivo* fluorescence, and chlorophyll *a* fluorescence emission analysis).

Materials and methods

Characterization of dendrimers

Amine-terminated G5 and G7 PAMAM dendrimers (hereinafter, G5 and G7, respectively) in methanol-free aqueous solutions, where G stands for generation, were provided by Dendritech Inc. (Midland, MI). The size distribution of nanoparticles was obtained using dynamic light scattering (DLS; Malvern Zetasizer Nano ZS, Malvern Instruments Ltd., Worcestershire, UK). ζ-potential was measured via electrophoretic light scattering (ELS) combined with phase analysis light scattering in the same instrument, using the lowest possible concentration yielding reproducible results (3.44 µM and 0.86 µM for G5 and G7, respectively). Size measurements were conducted at the concentration of 0.142 µM and 0.078 µM for G5 and G7, respectively, concentrations corresponding to those used during the bioassays. All the measurements were conducted at 28 ℃ both in pure water and in the exposure medium.

Cyanobacterial bioassay

Anabaena was routinely grown at 28 ℃ at a light intensity *ca.* 65 µmol photons $m^2 s^{-1}$ on a rotary shaker in 100 mL of AA/8+N which is an 8-fold dilution of the medium of Allen & Arnon (1955) supplemented with nitrate (5 mM) in 250 mL Erlenmeyer flasks. Exposure experiments were carried out in 20 mL of AA/8+N, in 50 mL Erlenmeyer flasks. The pH of the culture medium was adjusted to 7.4. Before exposure to dendrimers,

cultures were washed three times and resuspended in fresh culture medium to obtain a final optical density (DO_{750nm}) of 0.2. Commercial dendrimers stocks were diluted to a final concentration of 6.89 µM and they were sonicated for 15 min using an Ultrasonic bath (J.P. Selecta, Spain) before each bioassay. From these stocks, dendrimers were added to obtain the desired final bioassay concentrations. Cultures were exposed to increasing concentrations of G5 and G7 dendrimers (from 0.004 µM to 0.278 µM), for up to 72 h in a rotary shaker at 28 ℃ under constant illumination. Growth inhibition was calculated based on dry weight determination. The cells were collected, washed and dried at 70 ℃ for 24 h. The effective concentrations of dendrimers that caused 10%, 50% and 90% inhibition of the growth in terms of dry weight with respect to the control (EC_{10}, EC_{50} and EC_{90}, respectively) were calculated by the dose-response package (drc) using R Software, version 3.3.1. The concentration corresponding to the EC_{50} for each dendrimer was used to perform the mechanistic study of toxicity.

Optical and Transmission Electron Microscopy studies

For transmission electron micrographs, cyanobacterial cell suspensions exposed to G5 and G7 dendrimers were collected by centrifugation 3000 rpm for 1 min. Cells were prepared as described elsewhere[41]. Briefly, cells were fixed in agar blocks in 2.5% glutaraldehyde in buffer sodium cacodylate (50 mM) with $CaCl_2$ (5mM) for 1.5 h at 4 °C. Post-fixation was performed in osmium tetroxide into phosphate buffer for 2 h at 4 °C. Samples were dehydrated in ethanol and embedded in Durcupan resin (Fluka). Sample were sectioned in a Leica Reichert Ultracut S ultramicrotome, stained with uranyl acetate 2%. Ultrathin sections were visualized on a JEOL (JEM 1010) electron microscope (80 kV).

For morphological observations, cyanobacterial cells were collected by centrifugation at low relative centrifugal forces (1000 rpm) during 1 min in order to reduce the chance for artefacts. Observations of *Anabaena* filaments samples were carried out with a photomicroscope (BH2-RFCA; Olympus) equipped with phase-contrast and video camera systems (Leica DC Camera; Leica Microsystems).

Flow cytometry

Flow cytometry (FCM) analyses of *Anabaena* were performed after 72 h of exposure to the calculated EC_{50} of each dendrimer, using a Cytomix FL500 MPL flow cytometer (Beckman Coulter Inc., Fullerton, CA) equipped with an argon-ion excitation wavelength (488 nm), detector of forward (FS) and side (SS) light scatter and four fluorescence detectors corresponding to four

different wavelength intervals: FL1:525, FL2:575, FL3:620 and FL4: 675 (±20 nm).

For all cytometric parameters evaluated, at least 10000 events (cyanobacterial filaments) were analysed per culture; significant differences in fluorescence shifts were considered when it exceeded 5000 evaluated events. Since forward light scatter (FS) is correlated with the size or volume of a cell or particle and the side light scatter (SS) is correlated with the intracellular complexity[42] both parameters were used during the morphological analysis. Red autofluorescence (FL4), related to the chlorophyll a fluorescence emission, and FS histograms were used to characterize the cyanobacterial population in order to compare filaments of cells with similar length.

Seven physiological parameters were analysed by FCM: Intracellular ROS formation by using three different fluorochromes [H_2DCF DA as general ROS formation indicator, DHR 123 for hydrogen peroxide (H_2O_2) production and HE for superoxide ion ($O_2^{\bullet-}$) production]. Membrane integrity (PI), cytoplasmic membrane potential (DiBAC$_4$(3)), intracellular free Ca^{2+} (Calcium Green-1 AM) and intracellular pH (BCECF-AM).

The presence of oxidative DNA damage was detected by using the fluorescent OxyDNA assay. Cell suspensions were incubated with the corresponding fluorochromes at 25 ºC in darkness. Incubation times and other details concerning the fluorochromes used for FCM are given in Table S1. Data were collected using Kaluza software version 1.1 (Beckman Coulter).

Lipid peroxidation

Lipid peroxidation was determined in terms of thiobarbituric acid reactive substances (TBARS) following the protocol described by Ortega-Villasante *et al.*[42] with minor modifications[43]. Cyanobacteria cells were harvested by centrifugation (3000 rpm) and dissolved in 3 ml (0.67% w/v) trichloroacetic acid (TCA) solution and then broken by ultra-sonication at 400 mA for 120 s. The homogenate was centrifuged at 13.000 rpm for 30 min and 2 ml supernatant was mixed with 2 ml of 0.5% thiobarbituric acid (TBA) in 20% TCA. The mixture was heated in a hot block for 30 min, cooled to 25 ºC, and centrifuged at 13000 rpm for 5 min. The absorbance of the supernatant was measured at 532 nm. The value for nonspecific absorbance at 600 nm was subtracted.

The amount of TBARS was calculated by using the extinction coefficient of 155 mM^{-1} cm^{-1}. Lipid peroxidation was expressed as MDA content percentage with respect to the control.

Photosynthetic oxygen evolution and PSII activity

Oxygen evolution was measured at 28 ºC under saturating white light (300 µmol photons m^{-2} s^{-1}) with a Clark-type oxygen electrode (Hansatech) according to Leganés *et al.*[43]. Cells, washed and resuspended in HEPES 25 mM (pH 7.5), were supplemented with 5 mM NaHCO$_3$, pH 7.5.

Photosynthetic rates were corrected for chlorophyll a content and represented as percentage with respect to control. PSII activity in intact cells (15 µg Chl a mL^{-1}) was estimated as O$_2$ evolution in the presence of 2 mM phenyl-1,4-benzoquinone (PBQ), 10 mM CaCl$_2$ and 0.42 mM ferrycianide in saturating white light (300 µmol photons m^{-2}s^{-1}).

Photosynthetic pigment content and in vivo fluorescence

For the chlorophyll a and carotenoid determinations, samples were extracted in aqueous solution of methanol (90%, w/v) at 4 ºC for 24 h in darkness. The chlorophyll a and carotenoid content of the extract was estimated according to the spectrophotometric method[44]. For phycobiliprotein extraction, the cells (aliquots of 1 mL) were centrifuged 3 min at 13000 rpm and resuspended in 0.5 mL of phosphate buffer (pH 6), followed by three freeze-thawing cycles (immersion in liquid nitrogen and 6 min at 25 °C in a hot block) and subsequently by 15 min of ultra-sonication at 4 °C. To obtain a final volume of 1 mL, 0.5 mL of phosphate buffer (pH 6) was added, and the aliquots were stored 48 h at 4 °C. Finally, aliquots were centrifuged 10 min at 13000 rpm, and phycobiliprotein quantification was carried out spectrophotometrically, according to Lawrenz *et al.*[45]. *In vivo* fluorescence of the pigments was measured by transferring aliquots of 100 mL to an opaque black 96-well microtiter plate using a Fluorostar Omega plate reader (BMGLABTECH GmbH, Germany) essentially as described by Sobiechowska-Sasim *et al.*[45]. Fluorescence data were corrected for the corresponding pigment concentration. Each analysis was performed at least by triplicate.

Chlorophyll a fluorescence emission analysis

Chlorophyll a fluorescence emission was measured with a pulse amplitude modulated (PAM) fluorometer (Hansatech, Inc., Norfolk, UK). After dark adaptation of cells for 30 min to completely oxidize the PSII electron transport chain, the minimum fluorescence (F_0; dark adapted minimum fluorescence) was measured with weak modulated irradiation (1 µmol m^{-2} s^{-1}). Maximum fluorescence (Fm) was determined by the addition of DCMU (3-(3,4-dichlorophenyl)-1,1-dimethylurea) during actinic light illumination; the used concentration of DCMU (5 µM final concentration) was that necessary to permit the reduction of all PSII reaction centers[36,46]. Dark

adapted variable fluorescence (Fv) was calculated as $Fm - F_0$ and maximal PSII quantum yield as Fv/Fm. After the saturation flash, the cells were continuously irradiated with actinic light (200 µmol m^{-2} s^{-1}) and equilibrated for 60 s to record the steady-state fluorescence signal (Fs). Following this, a saturation flash (15800 µmol m^{-2} s^{-1} during 400 ms) was applied to measure the maximum fluorescence under light adapted conditions (Fm'); afterwards, actinic source was automatically switched off and 5 s far-red pulse was applied (to excite PS I activity and take out the electrons from the transport chain) and then, the light adapted minimal fluorescence yield (F_0') was measured. Next fluorescent parameters were calculated as follows: the maximum intrinsic PSII efficiency $Fv'/Fm' = (Fm' - F_0')/Fm'$, the effective PSII quantum yield; ϕPSII $= (Fm' - Fs)/Fm'$[47], the photochemical quenching coefficient; qP $= (Fm' - Fs)/(Fm' - F_0')$, the non-photochemical quenching coefficient; qN $= 1-(Fm'-F_0')/(Fm-F_0)$[48,49], and the vitality index Rfd $= (Fm - Fs)/Fs$[50].

Internalization analysis

Internalization studies were essentially performed as reported by Gonzalo et al.[31]. The Alexa Flour 488 reactive dye has a tetrafluorophenyl ester, which reacts efficiently with primary amines to form stable fluorescent dye-protein conjugates with excitation and emission maxima of 494 nm/519 nm. G5 and G7-PAMAM-Alexa Fluor 488 conjugates were prepared according to the standard protocol of the Alexa Fluor 488 microscale protein labelling kit (A30006, Molecular Probes), the procedure

parameters are listed in Table S3. In order to differentiate between surface bounds and truly internalized dendrimers, Anti-Alexa Fluor 488 Rabbit IgG Fraction (A-11094, Molecular Probes), was used. This antibody specifically links with Alexa488 dye producing a highly efficient quenching of the fluorescence signal. The amount and time of incubation of the Anti-Alexa Fluor 488 antibody were those reported by Gonzalo et al.[31].

Gene expression analysis by RT-qPCR

Total RNA was extracted from frozen cell pellets using hot acid (pH 4.5) phenol (Amresco LLC; VWR Chemicals, USA) at 65 ºC, followed by extraction with acid hot phenol:chloroform (1:1) and a second extraction with chloroform; subsequent treatment with 1 vol. isopropanol, centrifugation, pellet washing with 70% ethanol and resuspension in DEPC-treated water[51]. The remaining genomic DNA was removed using RQ1 RNase-Free DNase (Promega) for 30 min at 37 °C. Thereafter, RNA was purified using Trizol® (Invitrogen). The concentration of RNA was spectrophotometrically determined in a Nanodrop (Thermo Scientific). cDNA was synthetized from 1 µg of extracted RNA using the iScriptTM cDNA Synthesis Kit from Bio-Rad following manufacturer's instructions. RT-qPCR was performed on a Techne Quantica apparatus using SYBR Green Master mix (Roche); Table 1 list the primers used in this study as well as relevant information relative to each gene. The $2^{-\Delta\Delta CT}$ was used to normalize and calibrate transcript values with respect to the *rnpB* gene, suitable as cyanobacterial reference gene[48,52].

Table 1: Specific primers for RT-qPCR analysis.

Gene	Encoding	Primer sequence	Accession numbers
*sod*A	Mn Superoxide dismutase	F: 5'-GGTAACTCGGCTGGATTTGTA-3' R: 5'-AACGGTTTATTGGCTTTTTCA-3'	all0070
*sod*B	Fe superoxide dismutase	F: 5'-TCACTACGGCAAACATCACAA-3' R: 5'-CGGGCTTTAAAGAATTCCAGA-3'	alr2938
*prx*A	Peroxire-doxin	F: 5'-CTCCCGACTTTACAGCAACAG-3' R: 5'-GTGGGGCAAACAAAGGTAAA-3'	alr4641

Data analysis

Means and standard deviation values were calculated for each treatment from three independent replicate experiments. To determine significant differences between each treatment with respect to the corresponding control, data were statistically analysed conducting an overall one-way analysis of variance (ANOVA) using R software (version 3.3.1). A $p < 0.05$ was considered statistically significant. When significant differences were observed, means were compared using the multiple-range Tukey's HSD test.

Results

Physicochemical characterization of PAMAM dendrimers

The properties of amine-terminated G5 and G7 PAMAM dendrimers in pure water and in the culture medium (both in absence of cells) are listed in Table 2. The hydrodynamic diameter of the dendrimers was measured by DLS at the concentration corresponding to each EC$_{50}$ (*see Effect on the growth of cyanobacteria*) and through the size/number distributions. Two clear peaks around 5 and 8 nm were observed, for G5 and G7, respectively, in pure water, which is in good agreement with the data provided by the manufacturer. However, in culture medium the dendrimers presented aggregates whose size was 448 ± 48 and 416 ± 14 nm, for G5 and G7 dendrimers, respectively.

In the culture medium used, we could observe negatively charged aggregates with sizes in the 300–450 nm range, size that, as mentioned above, varied in the presence of dendrimers. This is most probably because of the heteroaggregation of positively charged dendrimers to the negative surface of the particles in the medium. The net charge of the dendrimer was analyzed by ELS, calculating the ζ-potential value in pure water and in culture medium; net charge presented by G5 and G7 dendrimers were clearly positive when suspended in the culture medium (+24 mV and +27 mV, respectively).

Table 2. Particle hydrodynamic size determined by dynamic light scattering, and ζ-potential measured by electrophoretic light scattering in pure water and in culture medium (AA/8+N) with their 95% confidence intervals.

Size (nm)		
	Pure water (pH 6.5)	AA/8+N (pH 7.4)
Without dendrimer	--	366 ± 89
G5	4.89 ± 0.58[a]	448 ± 48[a]
G7	7.93 ± 0.56[b]	416 ± 14[b]
ζ - Potential (mV)		
	Pure water (pH 6.5)	AA/8+N (pH 7.4)
Without dendrimer	-	-19.4 ± 1.28
G5	12.4 ± 2.38[c]	24.3 ± 1.07[c]
G7	22.4 ± 3.30[d]	27.4 ± 0.42[d]

[a] 0.142µM; [b] 0.78µM; [c] 3.44µM; [d] 0.86µM.

Effect on the growth of cyanobacteria

Table 3 lists the effective concentrations (EC) of G5 and G7 dendrimers that inhibit 10, 50 and 90% growth of the cyanobacterium *Anabaena*. Dose-response profiles of both dendrimers for *Anabaena* (from where the information in Table 2 was obtained) can be found in supplementary material Fig. S1. The data in Table 3 are given in terms of molarity (µM) in order to consider the large differences in molecular weight of both dendrimers when testing their toxicity (Table S2 shows the same information expressed in mass concentration units). Both dendrimers exerted clear toxicity towards *Anabaena*; however, the EC_{10}, EC_{50} and EC_{90} values of the G7 dendrimer were lower than those of the G5, indicating that higher generation G7 dendrimer was more toxic towards the cyanobacterium.

Table 3. Effective concentrations of G5 and G7 dendrimers that induced 10%, 50% and 90% of growth inhibition on *Anabaena* growth after 72 h and the model type fitted.

	Model fitted	EC_{10} (µM)	EC_{50} (µM)	EC_{90} (µM)
G5	W1.2	0.044 ± 0.009	0.142 ± 0.010	0.301 ± 0.036
G7	W1.3	0.012	0.078	0.255

		± 0.002	± 0.005	± 0.060

Effect on cell morphology and structure

The morphological characteristics of *Anabaena* filaments and cells were affected by 72 h of exposure to the assayed dendrimer concentrations. The results of the structural analysis through optical microscopy, TEM and FCM are compiled in Fig. 1. The filaments of *Anabaena* exposed to G5 and G7 dendrimers showed two clear morphological alterations: thickness increase and irregular shape morphologies in contrast with the control filament shape. Within filaments, cells acquired aberrant morphologies, they were distorted and vacuolated and in general they appeared as swollen and therefore bigger than control cells (Fig.1A, B and C).

Regarding ultrastructure, G5 dendrimers induce thylakoids disorganization, disrupted thylakoids membranes and gave rise to large polyphosphate granules formation (Fig. 1E and H); G7 dendrimers also induced the same thylakoid alterations and large polyphosphate granules formation but, additionally, cell envelope undulations could be observed, indicating envelope damage (Fig. 1I). In addition, FCM analysis revealed that dendrimers induced both, fragmentation of the filaments (roughly half size of the control), and an increase in the internal complexity (112% by G5 and 127% by G7); these alterations were more pronounced in the case of G7 dendrimer as may be seen in Fig.1J. This fragmentation was also observed by optical microscopy (Fig.S2).

Effects on the physiology of *Anabaena*

FCM allows the rapid and quantitative measurement of responses of individual *Anabaena* filaments to a toxic stress. Fig. 2 shows the results of physiological evaluation by FCM of *Anabaena* exposed to G5 and G7 dendrimers.

ROS formation

One of the most common responses of organisms to pollutants is the increase in intracellular ROS that can trigger an imbalance in their homeostasis and produce oxidative stress; as a result, they may compromise the integrity of cellular components such as membranes, photosynthetic apparatus or genetic material. Intracellular ROS level was analyzed by FCM using 3 different fluorochromes: H_2DCF DA (relatively non-specific probe that reveals formation of both, reactive oxygen and nitrogen species), DHR123 (reveals presence of $O_2^{\cdot-}$) and HE (reveals the presence of H_2O_2). As may be seen in Fig.2, H_2DCF DA revealed a clear ROS formation induced by both, G5 and G7 dendrimers; however, the induction was much higher when the culture was exposed to G7, which provoked a fluorescence increase of 304% with

respect to the control, than to G5, that induced an increase of 180% of the control ($p < 0.001$). Both dendrimers induced a similar increase of $O_2^{\bullet-}$ (around 160% of the control fluorescence), while G7 provoked a higher H_2O_2 formation as observed in the increase in HE fluorescence of 141% with respect to the control whereas upon G5 exposure, the fluorescence increase was of 112% ($p < 0.01$).
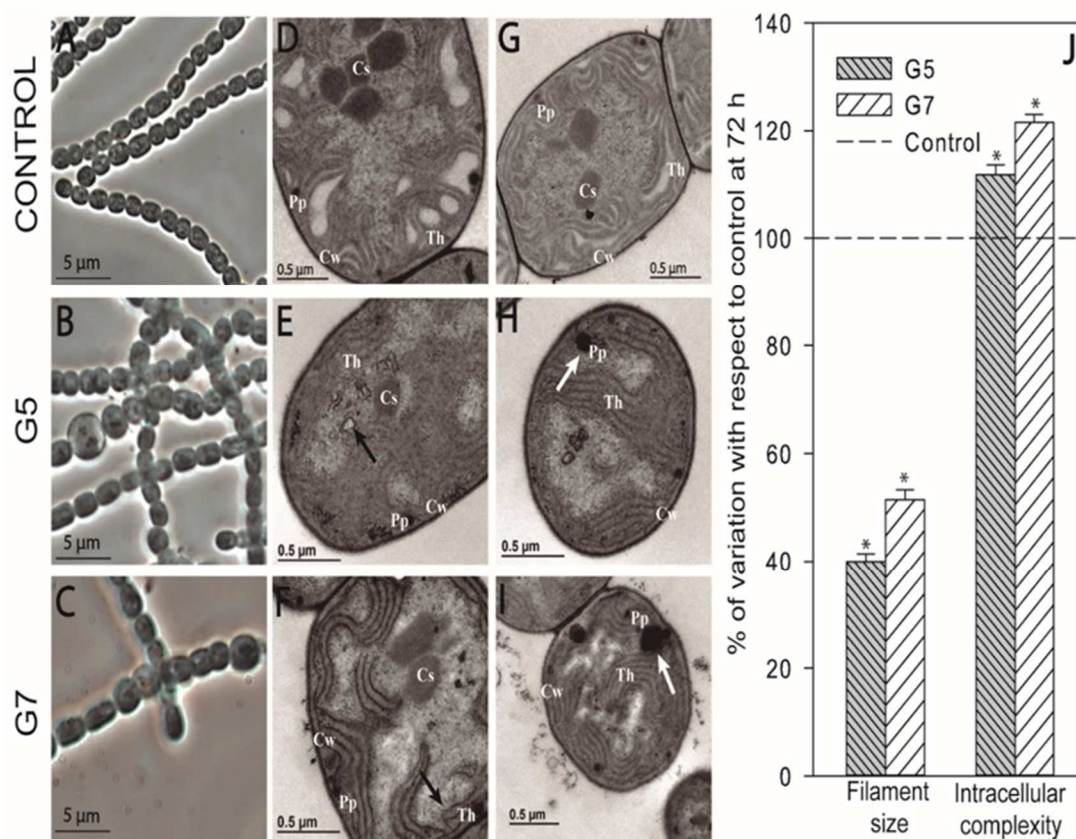
Figure 1. Morphological and ultrastructural studies of *Anabaena*, after 72 h exposure to EC$_{50}$ of G5 and G7 dendrimers, by optical microscopy (A, B and C show the shape of the filaments and cells within them). By TEM, images D and G are unexposed controls; E and F show the ultrastructural state of the thylakoid's membranes (black arrows indicate damaged thylakoids membranes) and H and I show larges polyphosphate granules (white arrows). By using flow cytometry image J shows the analysis of the filaments length and the internal complexity of the cells; these results are represented as percentage of variation of each parameter $\pm$ SD with respect to control (100% is indicated by the dashed line). Asterisks indicate treatments that are significantly different to the control (Tukey's HSD, $p < 0.05$). Cw: Cell wall; Th: Thylakoids membranes; Pp: Polyphosphate granules; Cs: Carboxysomes.

Oxidative DNA Damage

In view of the increase in ROS levels detected in *Anabaena* cells exposed to the dendrimers, we used FCM to further monitor the presence of 8-OHdG-DNA adducts by using the OxyDNA Assay kit (Fluorometric, Calbiochem) that contains a fluorescent binding protein with high affinity for 7,8-dihydro-8-oxo-2'-deoxyguanosine (8-OHdG), an important indicator of free radical-induced DNA damage. FCM analysis revealed that dendrimer exposure induced the formation of oxidative 8-OHdG adducts in the DNA of *Anabaena* (Fig. 2 and Fig. S3). As shown in Fig. 2, the levels of 8-OHdG adducts in cells treated with G5 were significantly increased till 248% ($p < 0.001$), whereas cells treated with G7 showed an increase of 455% ($p < 0.001$) in the formation of 8-OHdG residues both with respect to non-treated cells.

Cytoplasmic membrane integrity

Cell viability of *Anabaena* was significantly affected by the assayed dendrimer concentrations. Overproduction of ROS can trigger oxidative stress and this in turn may compromise the integrity of the cell membrane. Potential damage of the cytoplasmic membranes was analyzed from two different approaches. Firstly, PI was used since it is unable to pass through intact cell membranes (PI-). However, when integrity of cell membrane fails, PI is able to enter and stain nucleic acids (PI+), allowing to discriminate between those cells that emit fluorescence and therefore present damages in the cytoplasmic membrane and those in which the fluorochrome does not penetrate, no fluorescence is emitted and, therefore, cells maintain the integrity of the membrane[53]. Fig. 2 shows the fluorescence increase (PI+) with respect to the control. Membrane damage was more accused in the case of G7 exposed cultures which showed a fluorescence increase, by PI+ events, of around 500% ($p < 0.001$) whereas the cultures treated with G5 dendrimers showed around 300% ($p < 0.001$) of increase with respect to the control. Secondly, imbalances in intracellular ROS may lead to membrane damage by structural lipid peroxidation. The analysis was performed by quantification of TBARS (thiobarbituric acid reactive substances), that are end products of lipid peroxidation, predominantly malondialdehyde. Both dendrimers led to membrane lipid peroxidation. A significant increase of 300% ($p < 0.001$) of TABRS was observed in cultures treated with both G5 and G7 with respect to the control after 72 h of exposure

(Fig. 2). These results show a clear alteration in cytoplasmic membrane integrity.
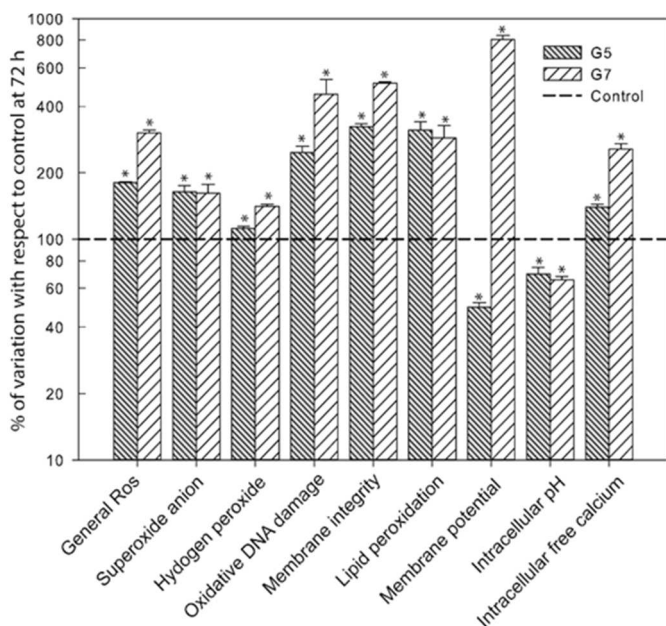
Figure 2. Physiological parameters analyzed in *Anabaena* after 72 h exposure to EC_{50} of G5 and G7 dendrimers by flow cytometry using a set of fluorochromes to evaluate each parameter: intracellular ROS balance by using 3 different fluorochromes (H_2DCF DA for general oxidative stress, DHR 123 for H_2O_2 production and HE for $O_2^{•-}$ production), the presence of oxidative DNA damage detected by using the fluorescent OxyDNA assay, membrane integrity (PI), cytoplasmic membrane potential (DiBAC$_4$(3), intracellular free Ca^{2+} (Calcium green-1 AM), intracellular pH (BCECF AM), metabolic activity (FDA) and. Results are represented as percentage of variation of the relevant physiological parameters ± SD with respect to control (100% is indicated by the dashed line). Asterisks indicate treatments that are significantly different to the control (Tukey's HSD, $p < 0.05$). Fig. S3 shows representative graphics from where these results were obtained.

Cytoplasmic membrane potential

The potential of the cytoplasmic membrane is mainly regulated by two factors: ionic membrane permeability and ionic transmembrane gradient. As mentioned above, G5 and G7 dendrimers compromised the integrity of the cytoplasmic membrane which may increase non-specific permeability causing membrane depolarization. Fig. 2 presents the results on cytoplasmic membrane potential after exposure of the cyanobacterium to G5 and G7. It was studied by FCM using the fluorochrome DiBAC$_4$(3); so that, cytoplasmic membrane depolarization will be reflected in an increased intracellular anionic dye concentration (increasing the fluorescence intensity), whilst a decrease in its accumulation will reflect hyperpolarization (decreasing fluorescence intensity). The cultures exposed to G7 showed a significant increase (depolarization) in fluorescence emission of ~ 800% with respect to the control ($p < $

0.001). In the case of G5, a decrease in fluorescence intensity (hyperpolarization), of ~ 50% with respect to the control, was observed [nevertheless a small population that had suffered a pronounced increase (depolarization) in fluorescence intensity when exposed to G5 was observed, denoted as R2 subpopulation in Fig. S3]; however, when the cells were exposed to higher concentrations of G5, no hyperpolarization was found, and a clear depolarization was observed (Fig. S4).

Intracellular free Ca^{2+}

Intracellular free calcium levels ($[Ca^{2+}]_i$) is a second messenger involved in signaling multiple environmental stresses in cyanobacteria: adaptation to heat and / or cold stress[54], response to salinity[54], differentiation of heterocysts[54] or response to pollutants[51,55]. The level of $[Ca^{2+}]_i$ was measured by FCM using the fluorochrome Calcium Green-1 AM. This fluorochrome is passively loaded into cells where it is cleaved to the cell-impermeant fluorescent product Calcium Green-1 which exhibits an increase in fluorescent emission intensity upon binding Ca^{2+} ion. As shown in Fig. 2, an increase in fluorescence was observed after dendrimer exposure; the induced increase was of 140% ($p < 0.001$) by G5 and 256% ($p < 0.001$) by G7 with respect to the control. Results indicated that exposure to G5 and, in a greater extent, to G7 caused a significant alteration of intracellular free Ca^{2+} homeostasis in the cyanobacterium.

Intracellular pH

The green/red BCECF fluorescence intensity ratio (green fluorescence is pH dependent whereas red fluorescence is pH independent) was used to measure intracellular pH in dendrimer exposed *Anabaena* by FCM. This ratio increases when intracellular pH increases and decreases when it decreases (within the physiological pH range). Fig. 2 shows the ratios (FL1/FL3) resulting from both treatments (with G5 and G7 dendrimers) with respect to the control ratio. The ratio significantly decreased in both cases, being 69% by G5 exposure, and 65% by G7 exposure, with respect to the control ($p < 0.001$). These decreases in green/red BCECF fluorescence intensity ratio imply an acidification of the intracellular pH upon 72 h exposure to both dendrimers, slightly more pronounced when exposed to G7.

Photosynthetic alterations

The parameters related to the photosynthetic process were studied upon exposure of cyanobacteria to dendrimers. Oxygen evolution provided an overview of the photosynthetic process. The analysis of the pigment content and their fluorescence provided general information

about the state of the photosynthetic apparatus. Fig. 3 shows the levels of oxygen evolution, PSII activity, pigment content and pigment fluorescence analysis in percentage with respect to the control values. To evaluate more deeply the mechanism of the effects of dendrimers on the photosynthesis, we performed chlorophyll a fluorescence emission analysis by PAM fluorimetry. Fig. 4 shows results obtained from PAM fluorimetry when *Anabaena* was exposed to G5 and G7 dendrimers, represented as percentage with respect to the control values for each measured/calculated parameter.

Oxygen evolution

Oxygen evolution of the cyanobacterium exposed to the EC_{50} of both G5 and G7 dendrimers is shown in Fig. 3. The cyanobacterium showed a significant decrease in the oxygen evolution after 72 h of exposure to both dendrimers. These reductions in oxygen evolution induced by G5 and G7, was similarly around 50% (μmol O_2 mg chl^{-1} h^{-1}) with respect to the control ($p < 0.001$).

PSII activity

The observed decrease in oxygen evolution under both dendrimer exposure could reflect an effect on the activity of the PSII. As shown in Fig. 3, there was a significant decrease in PSII activity; when exposed to G5 and G7 dendrimers, the PSII activity was around 50% and 40% ($p < 0.001$), respectively, with respect to the PSII activity observed in the control.
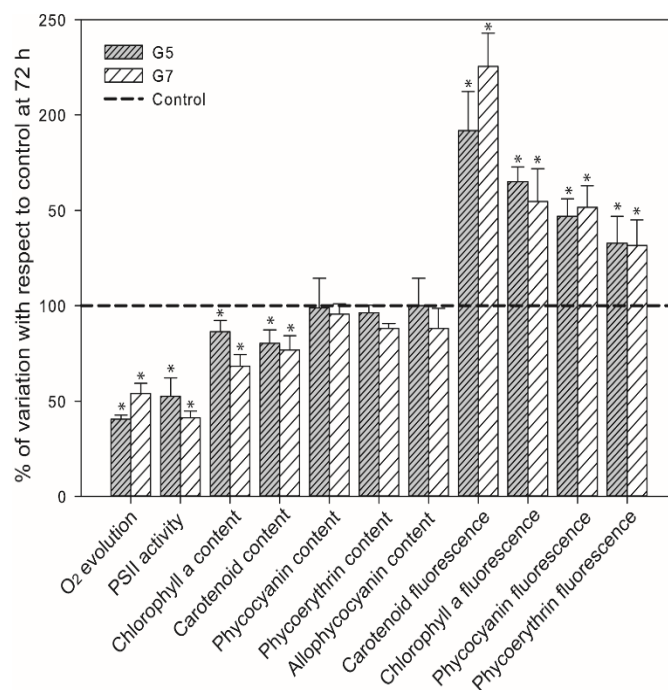
Pigment content

Anabaena pigment contents were quantified upon exposure to the EC_{50} of each dendrimer. The exposure caused a reduction in chlorophyll a concentration, so that, treated cultures presented a content of 86% and 68% ($p < 0.01$), with respect to the control, when exposed to G5 and G7, respectively. Regarding carotenoid content, G5 and G7 caused a similar decrease with a content of 80% and 76%, respectively, with respect to the control. The rest of the photosynthetic pigments did not significantly vary with respect to the control; however, slight phycocyanin, phycoerythrin and allophycocyanin content decrease could be observed on G7 treated cultures (Fig. 3).

In vivo pigment fluorescence measurements

The presence of both dendrimers induced a general increase of the *in vivo* photosynthetic pigment fluorescence with respect to the control. *In vivo* carotenoid fluorescence increase was higher by G7 exposure than by G5, (226% and 192%, respectively, with respect to the control, $p < 0.01$).

The observed increase in chlorophyll a fluorescence was similar between G5 and G7 exposure (165% and 155%, respectively, with respect to the control, $p <$

0.01). Similarly, phycocyanin and phycoerythrin showed an *in vivo* fluorescence increase when exposed to G5 (147% and 132%, respectively, $p < 0.01$) and to G7 (152% and 132%, respectively, $p < 0.01$), both with respect to the control.


Figure 3. Photosynthetic apparatus related parameters studied in *Anabaena* after 72 h exposure to EC_{50} of G5 and G7 dendrimers: oxygen evolution, PSII rate, chlorophyll a and accessory pigment content and fluorescence level (measured *in vivo*). Results are represented as percentage of variation of each parameter ± SD with respect to control (100% is indicated by the dashed line). Asterisks indicate treatments that are significantly different to the control (Tukey's HSD, $p < 0.05$)

Chlorophyll a fluorescence emission analysis

As already shown, O_2 evolution and PSII activity were impaired in *Anabaena* exposed to G5 and G7 dendrimers. In order to further elucidate which of the different photosynthetic events in *Anabaena* was altered by the dendrimers, chlorophyll a fluorescence emission analysis was performed (*F*ig.4).

A clear alteration in all the chlorophyll a related parameters studied was observed after G5 and G7 dendrimer exposure; these alterations were similar for both treatments. The dark-adapted minimum fluorescence, F_0, significantly increased in both cases (120% with respect to the control). The maximum fluorescence, Fm, did not show any significant variation upon dendrimer exposure. However, a significant increase in the steady-state fluorescence, Fs, of around 140% with respect to the control, was observed. Rfd, also termed the "vitality index", showed a significant lower value of around 40% with respect to the control; this

parameter is accepted as a measure of stress effects on PSII[56] so in this case, Rfd is probably revealing alteration in the photosynthesis. The dark adapted

Fv/Fm reflects the maximum potential of PSII quantum yield; this ratio slightly decreased after both treatments (only significant in the case of G5 dendrimer), but it
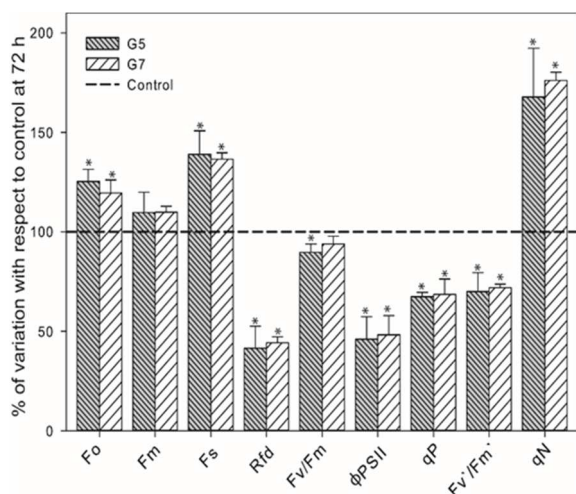

Figure 4. Chlorophyll *a* fluorescence emission parameters of *Anabaena* after 72 h exposure to EC_{50} values of G5 and G7 dendrimers. Dark adapted minimum fluorescence(F_0), dark adapted maximum fluorescence (Fm; measured using DCMU), steady-state fluorescence signal (Fs), maximum efficiency of PSII photochemistry (Fv/Fm), the maximum intrinsic PSII efficiency (Fv'/Fm'), the effective PSII quantum yield (ɸPSII), the photochemical quenching coefficient (qP), the non-photochemical quenching coefficient (qN), and the vitality index (Rfd). Results are expressed as percentage of variation of relevant fluorescence parameters ± SD with respect to control (100% is indicated by the dashed line). Asterisks indicate treatments that are significantly different to the control (Tukey's HSD, $p < 0.05$).

seems not to be a sensitive indicator of the toxicity exerted by G5 and G7 dendrimers. The effective quantum yield of PSII, ɸPSII, is used as a general indicator of plant stress physiology[47]. This ratio is an estimate of the effective portion of absorbed quanta used in PSII reaction centers: it is affected by the proportion of open, oxidized PSII reaction centers (estimated by the so-called photochemical quenching or qP) and also by the intrinsic PSII efficiency (estimated as the Fv'/Fm' ratio)[47]. As shown in *F*ig.4, ɸPSII values were roughly, for both dendrimers, half of that of the control (45%, p < 0.01), which correlates well with the decreases observed in Fv'/Fm' whose values, upon dendrimers exposure, were around 68% of that of the control and those observed in qP which also were, in both cases, around 67% (p < 0.01) of control value. In agreement, non-photochemical quenching, qN, that is mainly ascribed to state transition[57,58] or thermal dissipation[59], significantly increased with respect to the control after G5 and G7 dendrimers exposure (168% and 176%,

respectively) dissipating an important quantity of energy that is not used in the photochemical process.

Effect of dendrimers exposure on transcription of selected genes involved in oxidative stress defense

Several environmental conditions as well as different pollutant may trigger an imbalance of intracellular ROS production in many organisms, however, photosynthetic organisms do not only need to manage the oxidative stress generated by ROS produced in the same way as heterotrophic organisms, but also that produced during photosynthetic electron transport. In order to avoid oxidative damage, organisms have developed different mechanisms that regulate their concentration, by turning them into innocuous compounds; thus, these mechanisms have to be in balance with ROS formation in order to avoid oxidative stress[60].
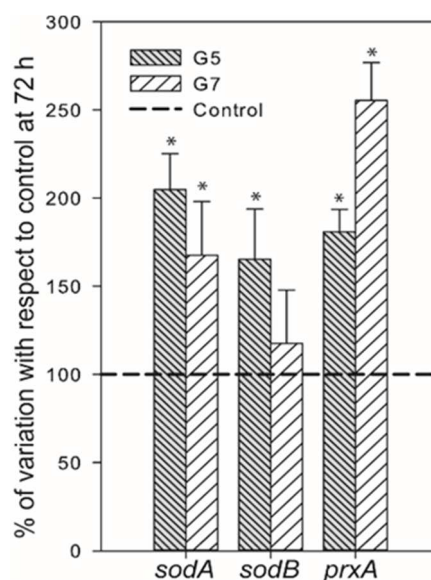
Figure 5. Effect of G5 and G7 dendrimers on expression of genes involved in oxidative stress defense, after 72 h exposure. Data are represented as percentage of gene expression with respect to the control. Asterisks indicate treatments that are significantly different to the control (Tukey's HSD, $p < 0.05$).

RT-qPCR was used to determine changes in the expression level of three genes encoding proteins involved in oxidative stress regulation after 72 h of exposure of *Anabaena* to G5 and G7 dendrimers. Results have been represented as percentage of expression with respect to the control (Fig. 5). A clear increase in the expression of the three evaluated genes was observed; expression level of *sodA* (encoding Mn superoxide dismutase) was significantly higher than that of control cells, slight more pronounced in the case of G5 than G7 dendrimer (205% and 168%, respectively, with respect to the control). Similarly, *sodB* (encoding Fe superoxide dismutase) showed an increase of

165% and 117%, respectively, when *Anabaena* was exposed to G5 and G7 dendrimers. The gene *prxA*, encoding a peroxiredoxin, showed even higher levels of expression under both treatments, with respect to the control; furthermore, this increase of expression was clearly higher when exposed to G7 (*prxA* expression increased to 255% with respect to the control) than to G5 dendrimer (*prxA* expression increased to 181%).

Dendrimer internalization

It has been found that dendrimers are internalized in different human and environmental cell systems (for a recent review see Naha et al.[61]). In order to study whether PAMAM dendrimers were internalized in the cyanobacterium, we conjugated G5 and G7 dendrimers with Alexa Fluor 488 to get green-labeled PAMAM dendrimers. The Alexa Fluor conjugates may be detected by confocal microscopy. In order to discriminate between cell dendrimer internalization and cell-surface bound dendrimers, we used a specific antiAlexa 488 antibody. The antibody does not cross cellular membranes and upon binding, the fluorescence of cell-surface bound Alexa Fluor 488- dendrimer conjugates is quenched, so that only conjugates internalized into the cell are visualized.

Figure 6 shows confocal micrographs of internalized Alexa-dendrimer conjugates in representative cyanobacterial filaments. In the case of G5, the dendrimers have been internalized in almost all filament cells and distributed mainly in the center of the cell where denser green-fluorescent spots are observed. In the case of G7, the dendrimers did not clearly internalize in all cells of the filament as observed in G5. In some of the cells, dense green granules could be seen in the center but also in distal parts of the cells. In other cells, green fluorescence was fainter with some accumulation near the internal layer of the cell envelope. It is noticeable that in the case of G7, those cells with greater internalization did not show chlorophyll fluorescence (see also the overlay image), indicating that those cells were severely affected. This strongly correlates with the higher toxicity induced by this dendrimer in the cyanobacterium and with the observed decrease in chlorophyll content, inhibition of photosynthesis and higher degree of disorganization of thylakoid membranes. In the case of G5, some degree of dendrimer localization in or near photosynthetic membranes occurred as shown by the yellow color of the overlay images. This could also reflect the damage on the photosynthetic apparatus caused by this dendrimer although cells as severely affected as those exposed to G7 were not observed, further corroborating that G5 is less toxic than G7.

Discussion

To date, several studies of the biological effects of PAMAM dendrimers in different cell systems have concluded that their toxicity is dependent on generation (size), dose, exposure time, core and surface functionalization with different groups[19–24,31]. Most of them have been performed towards animal or human cells given the biomedical interest of dendrimers[62,63]; thus, there are not many studies in the literature concerning the toxicity of PAMAM dendrimers on organisms of environmental relevance[22,25–31]. However, their wide range of potential applications has raised awareness towards their release into the environment and potential effects on relevant aquatic organisms; in fact, biodistribution studies have found that PAMAM dendrimers are found in urine of rabbit and mouse models exposed to them[6464]. PAMAM dendrimers may reach the aquatic environment being carried by urine, which may affect aquatic biota as relevant as cyanobacteria, which as primary producers are at the base of the trophic chain. In fact, only one tested low generation dendrimers towards cyanobacteria as model organisms[31]. In the present study, a detailed toxicological analysis was performed upon 72 h exposure of the cyanobacterium *Anabaena* to cationic G5 and G7 dendrimers. The obtained EC_x values are lower than those obtained by Gonzalo *et al.*[31] who tested cationic G2, G3, and G4 dendrimers towards *Anabaena* sp PCC 7120, therefore, maintaining the trend of higher toxicity for higher dendrimer generation. Previous studies showed a correlation between the positive charge of the dendrimers and their increased toxicity[21,29,31]. The harm results from the interaction of their primary surface amines with the negative charged molecules present in the cell membranes, destabilizing them and sometimes causing cell lysis[65]; in agreement, our results show that G7, which presents higher positive surface net charge, induced more damage at membrane level as widely discussed below. As both dendrimers resulted to be toxic towards the cyanobacterium, a thoroughly study to understand the toxic mechanism of action was performed.

Since cyanobacteria are able to perform oxygenic photosynthesis, they are more susceptible to suffer oxidative stress than other prokaryotes. In the present study, one of the main biological effects observed is that dendrimer exposure triggered imbalances in ROS formation. The same has been previously reported by Naha *et al.*[23] and Mukherjee *et al.*[19] who tested G4-G6 towards different cell lines, by Petit *et al.*[30] when tested G4 toward *Chlamydomonas reinhardtii* and by Gonzalo *et al.*[31] when tested G2-G4 towards *C. reinhardtii* and *Anabaena*. In this regard, treatments with G5 and G7 dendrimers induced a clear imbalance in ROS formation revealing higher toxicity by the exposure to the highest generation dendrimer. Results of gene expression is consistent with ROS imbalance after 72 h of dendrimers exposure. The expression of both superoxide dismutase genes (*sodA* and *sodB*), that may

be correlated to the increase of intracellular $O_2^{\bullet-}$ level, were higher than the control ones; similarly, peroxiredoxin gene (*prxA*) showed clear overexpression when exposed to the dendrimers, specially to G7, which is consistent given the observed H_2O_2 overproduction. ROS high reactivity may affect many cell structures inducing filament fragmentation, thylakoids membrane disruption through lipid peroxidation[66,67], losses in pigment content and in membrane integrity[68] as well as alteration in the photosynthetic apparatus[60]. In this regard, inherent cell properties analyzed were similarly
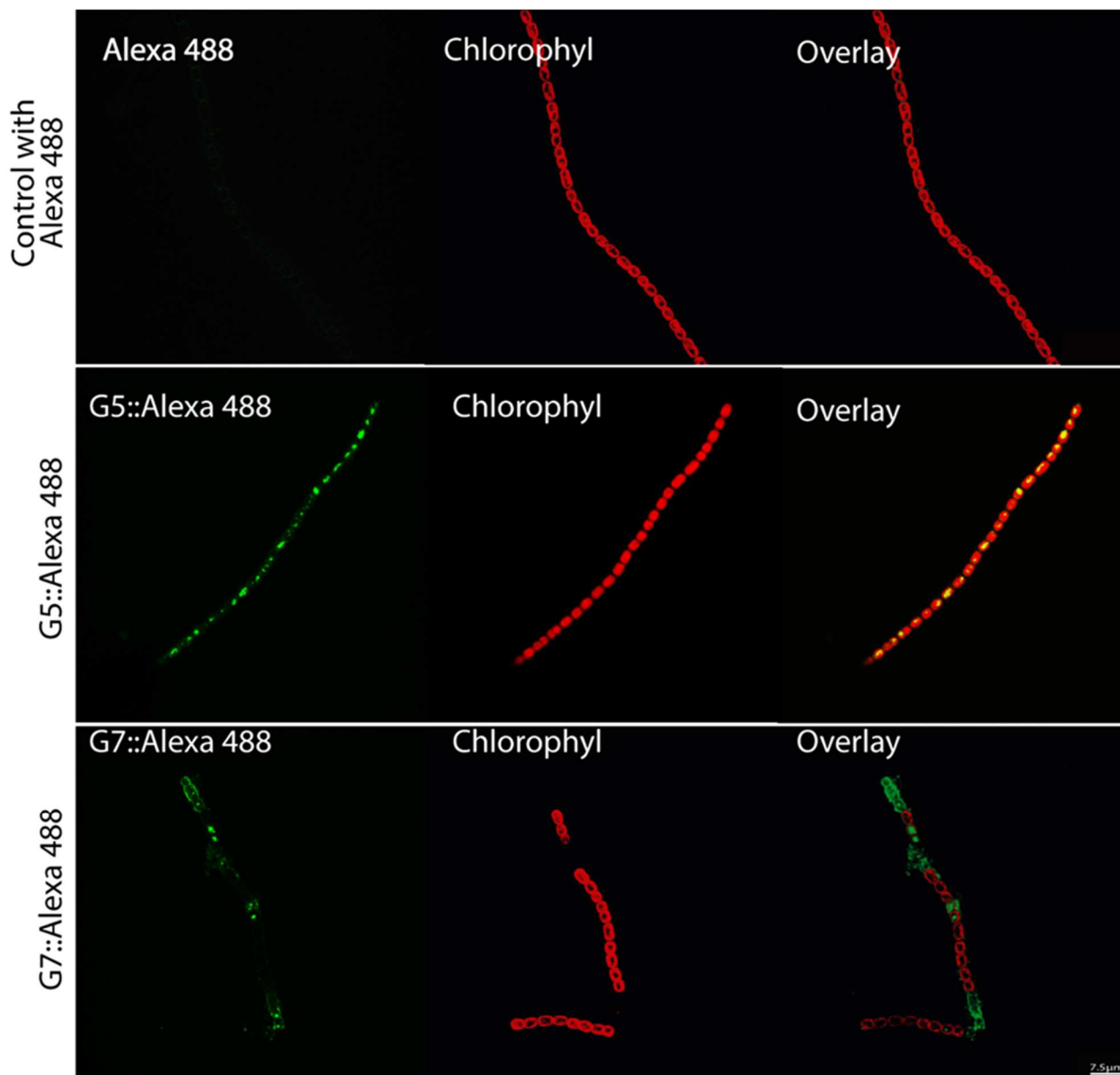
Figure 6: internalization of G5 and G7 PAMAM dendrimers conjugated to Alexa Fluor 488 in *Anabaena* PCC7120 cells after 72h incubation. Images are (left to right): Dendrimer::Alexa 488-conjugated fluorescence (green), chlorophyll *a* fluorescence (red) and overlay red/green fluorescence.

affected by exposure to G5 and G7 dendrimers. A decrease in filament size was observed (as described by Gonzalo *et al.*[31] in the presence of lower generation dendrimers), accompanied by an increase of internal complexity; possible consequence of the damage and disorganization of the intracellular structures (such as thylakoid disruption) which may be produced by the increase in ROS as described by Prado *et al.*[69].

ROS are thought to induce spontaneous damage to DNA; thus, the potential genotoxic mode of action of dendrimers was studied. Oxidative attack on DNA results in mutagenic structures such as 8-hydroxyadenine and 8-hydroxyguanine, which induce instability of repetitive sequences. Oxidative DNA damage in *Anabaena* cells exposed to dendrimers was analyzed via the formation of 8-OHdG by FCM. Results showed that dendrimers significantly increased oxidative DNA damage in

exposed *Anabaena* cells with respect to the untreated control, with G7 as the most damaging. It has already been reported that G4, G5 and G6 PAMAM dendrimers induce DNA damage in the fish cell line PLHC-1 although no 8-OHdG adducts were found[70]. Also G2 and G3 cationic phosphorus dendrimers have been reported to cause DNA damage in murine embryonic hippocampal cells[71]. As far as we know, this is the first report that provides quantitative measurements of oxidative DNA damage in cyanobacterial cells exposed to environmental contaminants, indicating that oxidative stress is a likely cause of dendrimer genotoxicity in *Anabaena* (ROS-mediated DNA oxidation).

Moreover, ROS may damage membranes and an abrupt increase in membrane non-specific permeability prevents an appropriate maintenance of the ionic transmembrane gradient inducing

membrane depolarization as seen upon G7 exposure, as previously reported by Geitner et al.[72] when tested cationic G4 dendrimers on the soil amoeba *Dictyostelium discoideum*. The hyperpolarization of the membrane, observed upon G5 exposure at the EC_{50}, is puzzling and probably related with the interaction between this specific cationic dendrimer and the cytoplasmic membrane surface. However, at higher effective concentrations, hyperpolarization was not present, and a clear depolarization was observed indicating also extended damage to the cytoplasmic membrane induced by G5 albeit at higher concentrations than in the case of G7. Consistently, the observed increase in $[Ca^{2+}]_i$, meaning loss of its homeostasis, has been correlated to the response under different stress conditions[51,54,55] in order to maintain physiological functions under intracellular acidification[73]; an increase in $[Ca^{2+}]_i$ after exposure of green algae *C. reinhardtii* to Triclosan (antibacterial compound) was also observed accompanied by intracellular acidification and ROS overproduction[51].

Previous studies with cationic G4 towards *C. reinhardtii* have shown oxygen evolution stimulation triggered by dendrimer exposure, although several genes involved in photosynthesis were downregulated[30]. Gonzalo et al.[31] also observed ROS overproduction in *Anabaena* exposed to cationic G4 but it seemed not to be related with damages in the photosynthetic apparatus since the specific location of ROS (observed by confocal microscopy using H$_2$DCF DA) was not on the photosynthetic membranes and chlorophyll *a* fluorescence emission analysis did not reveal any alteration on photosynthetic parameters. Petit et al.[25] tested G5 cationic PAMAM dendrimers with *C. reinhardtii* but did not observe significant alteration on oxygen evolution, however, it must be noted that they used lower concentrations than those used in this study. As an overview of the photosynthetic process and their linkage with global metabolism, we observed a clear reduction in oxygen evolution induced by G5 and G7. The evaluation of the PSII activity supported this result since the mentioned decrease in oxygen evolution correlated well with the observed decrease in PSII activity. Furthermore, in the present study, dendrimer exposure triggered a reduction in chlorophyll *a* and carotenoids content which have been correlated with a decrease in oxygen evolution after exposure of *Anabaena* to cerium nanoparticles[31] and after exposure of *Lemna minor* and *Scenedesmus obliquus* to flumioxazin[74]. Chlorophyll *a* fluorescence emission analysis seems to reflect a similar interaction between both dendrimers and the photosynthetic apparatus. Although Misumi et al.[75]. showed how *F*v/*F*m correlates well with alterations in phycocyanin

content and therefore, the slight decrease in *F*v/*F*m may be related with the slight phycocyanin content alteration, *F*v/*F*m seems not to be a sensitive indicator of dendrimer toxicity in cyanobacteria. The increase in F_0 is characteristic of the destruction of PSII reaction centers or the impairment of transfer of excitation energy from antennae to the reaction centers in higher plants[76]; in cyanobacteria, this increase may suggest phycobilisomes decoupling from PSII in order to downregulate photosynthetic activity by dissipating energy transferred to the reaction centers[77]; this is also corroborated by the increase of the *in vivo* fluorescence of phycobiliproteins. The increase in *F*s indicates an increase in the number of non-active PSII centers, and this is further supported by the observed and significant decrease in qP, which indicates that the number of open/active PSII reaction centers are diminished upon exposure to the dendrimers. This is consistent with the reduction observed in ɸPSII, that is used as a general indicator of plant stress physiology[47]. This parameter estimates the effective portion of absorbed energy used in PSII reaction centers; it is affected by the proportion of open, oxidized PSII reaction centers, estimated by qP, and also by the intrinsic PSII efficiency, estimated as the *F*v'/*F*m' ratio[46,47]. On the other hand, energy dissipation was estimated by qN (or NPQ) which shows a clear increase evidencing a mechanisms of energy dissipation. As an overview, a reduction in vitality index value (Rfd) has been linked with a measure of stress effects on PSII physiological state[36,78]; in this regard, the increase observed in *in vivo* chlorophyll *a* fluorescence, produced by both dendrimers, may be related with an interruption of the electron transport at the acceptor side of the PSII[79] which is consistent with the reduction observed in oxygen evolution and with the mentioned decrease in ɸPSII.

We report that G5 and G7 cationic PAMAM dendrimers (in Alexa-dendrimer conjugates) were largely internalized by the cyanobacterium. G5 was internalized in most cells in the filament and, most of the green fluorescence localized in the center of the cells where dense green spots could be observed. However, not all cells in the filament exposed to G7 took up the dendrimer and, interestingly, the cells showing the highest green fluorescence did not show chlorophyll fluorescence, indicating that these cells with highly internalized G7 were severely affected. The fact that G7 did not enter in all cells could be due to its higher molecular weight, which might slow the process of internalization. Our group already reported internalization of G2, G3 and G4 cationic-PAMAM dendrimers in *Anabaena* and the green alga *Chlamydomonas reinhardtii*[31] with no clear affection of photosynthetic membranes. Efficient

dendrimer internalization has been found in studies in human cell lines. Differences in residence times in the cell membranes have been observed and were linked to differences in membrane chemical composition; thus, in addition to molecular size certain factors such as specific modulation of cell membrane by dendrimers might also be involved in their permeability[80,81]. In addition, the pH of the surrounding media may affect their internalization[82]. It is not yet clear how PAMAM dendrimers cross the plasma membrane. In eukaryotes, it has been reported that dendrimers may be taken up by endocytosis and micropinocytosis (see Naha et al.[61] for a review). Direct penetration might also happen, dendrimers may produce nanoholes on lipid bilayers by direct interaction[20,65,83–85], or damage the membrane, indirectly, through the induction of ROS overproduction and subsequently lipid peroxidation[66] which may cause membrane permeabilization. In this context, endocytosis is not likely to occur in cyanobacteria due to their prokaryotic nature, although, it has been suggested that cyanobacteria use classical endocytosis and macropinocytosis to internalize exogenous GFP[81]. G5 and G7 PAMAM dendrimers both impaired membrane integrity and altered membrane potential, although these alterations were more evident with G7; thus, it is likely that both dendrimers might internalize in cyanobacteria by direct penetration due to altered membrane permeability. The fact that cationic PAMAM dendrimers of higher size such as G5 and G7 are efficiently internalized by organisms of high ecological relevance in aquatic ecosystems such as cyanobacteria poses a serious environmental issue due to the observed cytotoxicity.

Our data suggest that in the cyanobacterium, high generation G5 and G7 dendrimer exposure results in oxidative stress, which triggers many physiological alterations including oxidative DNA damage. Furthermore, despite no negative effect on photosynthesis was observed upon exposure of *Anabaena* to G2, G3 and G4 PAMAM dendrimers, the photosynthetic activity of the cyanobacterium was clearly affected by high generation G5 and G7 dendrimers, compromising the sustainability of the aquatic ecosystem.

Conclusions

In short, both dendrimers showed relevant toxicity towards *Anabaena* sp. PCC7120, causing structural and physiological alterations. Both dendrimers triggered pronounced ROS overproduction and subsequently induced cell envelope disruption, followed by alterations in membrane potential and intracellular pH, $[Ca^{2+}]_i$ homeostasis and oxidative DNA damage. Remarkably, several photosynthetic related parameters such as the photochemical event

or pigment contents were also affected, in parallel, by the dendrimers. These kinds of damages may lead to a severe metabolism shifts of the cyanobacterium affecting their ecological function. G7 dendrimer was more toxic than G5 when evaluating most of the physiological parameters. The study has revealed how high generation dendrimers have induced photosynthetic damages which had not previously been described. Both dendrimers were internalized into *Anabaena* cells; the pattern of internalization varied between both dendrimers, with G5 internalized in most cells in the filament, whereas G7 did not internalize in all cells in the filament but when internalized, cells were severely affected. Overall, cationic high generation PAMAM dendrimers may cause relevant environmental damages, since they clearly affect primary producers, such as cyanobacteria, a relevant organism in aquatic ecosystems. These findings may help in safer-by design strategies in the manufacturing of dendrimers.

References

1. Kaur, D., Jain, K., Mehra, N. K., Kesharwani, P. & Jain, N. K. A review on comparative study of PPI and PAMAM dendrimers. *J. Nanoparticle Res.* **18,** 146 (2016).
2. Bosman, A. W., Janssen, H. M. & Meijer, E. W. About Dendrimers: Structure, Physical Properties, and Applications. *Chem. Rev.* **99,** 1665–1688 (1999).
3. Maiti, P. K., Çağin, T., Wang, G. & Goddard, W. A. Structure of PAMAM dendrimers: Generations 1 through 11. *Macromolecules* **37,** 6236–6254 (2004).
4. Labieniec-Watala, M., Karolczak, K., Siewiera, K. & Watala, C. The janus face of PAMAM dendrimers used to potentially cure nonenzymatic modifications of biomacromolecules in metabolic disorders - A critical review of the pros and cons. *Molecules* **18,** 13769–13811 (2013).
5. Kesharwani, P., Jain, K. & Jain, N. K. Dendrimer as nanocarrier for drug delivery. *Prog. Polym. Sci.* **39,** 268–307 (2014).
6. Gkika, D. A. *et al.* Nano-patents and Literature Frequency as Statistical Innovation Indicator for the use of Nano-porous Material in Three Major Sectors: Medicine, Energy and Environment. *J. Eng. Sci. Technol. Rev.* **9,** (2016).
7. Kaphle, A., Navya, P. N., Umapathi, A. & Daima, H. K. Nanomaterials for agriculture, food and environment: applications, toxicity and regulation. *Environ. Chem. Lett.* **16,** 43–58 (2018).
8. Fulda, C., Weber-Bruls, D. & Werth, J. Nano is

nano is nano or: Nanotechnology - A European legal perspective. *Nanotechnol. Rev.* **3,** 401–409 (2014).

9. Otto, D. P. & de Villiers, M. M. Poly(amidoamine) Dendrimers as a Pharmaceutical Excipient. Are We There yet? *J. Pharm. Sci.* **107,** 75–83 (2018).

10. McMahon, M. T. & Bulte, J. W. M. Two decades of dendrimers as versatile MRI agents: a tale with and without metals. *Wiley Interdiscip. Rev. Nanomedicine Nanobiotechnology* e1496 (2017). doi:10.1002/wnan.1496

11. Sk, U. H. in *Antimicrobial Nanoarchitectonics* (ed. Grumezescu, A. M.) 323–355 (Elsevier, 2017).

12. Alighardashi, A. Development and Application of Graphene Oxide / Poly-Amidoamines Dendrimers (GO / PAMAMs) Nano-Composite for Nitrate Removal from Aqueous Solutions. (2018).

13. Diallo, M. S., Christie, S., Swaminathan, P., Johnson, J. H. & Goddard, W. A. Dendrimer enhanced ultrafiltration. 1. Recovery of Cu(II) from aqueous solutions using PAMAM dendrimers with ethylene diamine core and terminal NH 2 groups. *Environ. Sci. Technol.* **39,** 1366–1377 (2005).

14. Gopalakrishnan, I., Samuel, R. S. & Sridharan, K. in *Emerging Trends of Nanotechnology in Environment and Sustainability* (ed. Karthiyayini Sridharan) 89–98 (Springer, 2018).

15. Deraedt, C., Melaet, G., Ralston, W. T., Ye, R. & Somorjai, G. A. Platinum and Other Transition Metal Nanoclusters (Pd, Rh) Stabilized by PAMAM Dendrimer as Excellent Heterogeneous Catalysts: Application to the Methylcyclopentane (MCP) Hydrogenative Isomerization. *Nano Lett.* **17,** 1853–1862 (2017).

16. Ou, G. *et al.* Fabrication and application of noble metal nanoclusters as optical sensors for toxic metal ions. 2485–2498 (2018).

17. OECD, Series on the Safety of Manufactured Nanomaterials, No. 27 List of manufactured nanomaterials and List of endpoints for Phase one of the sponsorship programme for the testing of manufactured nanomaterials: Revision, Env/Jm/Mono 46. (2010).

18. OECD. Dossier on dendrimers. Series on the Safety of Manufactured Nanomaterials No. 46 ENV/JM/MONO(2015)9. (2015).

19. Mukherjee, S. P., Lyng, F. M., Garcia, A., Davoren, M. & Byrne, H. J. Mechanistic studies of in vitro cytotoxicity of poly(amidoamine) dendrimers in mammalian cells. *Toxicol. Appl. Pharmacol.* **248,** 259–268 (2010).

20. Jain, K., Kesharwani, P., Gupta, U. & Jain, N. K. Dendrimer toxicity: Let's meet the challenge. *Int. J. Pharm.* **394,** 122–142 (2010).

21. Malik, N. *et al.* Dendrimers: Relationship between structure and biocompatibility in vitro, and preliminary studies on the biodistribution of125I-labelled polyamidoamine dendrimers in vivo. *J. Control. Release* **65,** 133–148 (2000).

22. Fernández Freire, P., Peropadre, A., Rosal, R., Pérez Martín, J. M. & Hazen, M. J. Toxicological assessment of third generation (G3) poly (amidoamine) dendrimers using the Allium cepa test. *Sci. Total Environ.* **563–564,** 899–903 (2016).

23. Naha, P. C., Davoren, M., Lyng, F. M. & Byrne, H. J. Reactive oxygen species (ROS) induced cytokine production and cytotoxicity of PAMAM dendrimers in J774A.1 cells. *Toxicol. Appl. Pharmacol.* **246,** 91–99 (2010).

24. King Heiden, T. C., Dengler, E., Kao, W. J., Heideman, W. & Peterson, R. E. Developmental toxicity of low generation PAMAM dendrimers in zebrafish. *Toxicol. Appl. Pharmacol.* **225,** 70–79 (2007).

25. Petit, A. N., Eullaffroy, P., Debenest, T. & Gagné, F. Toxicity of PAMAM dendrimers to Chlamydomonas reinhardtii. *Aquat. Toxicol.* **100,** 187–193 (2010).

26. Blaise, C., Gagné, F., Auclair, J., Maysinger, D. & Sutthivaiyakit, P. Ecotoxicity of a potential drug nano-formulation: PAMAM-dendrimer and minocycline. *J. Xenobiotics* **4,** 85–87 (2014).

27. Naha, P. C., Davoren, M., Casey, A. & Byrne, H. J. An ecotoxicological study of poly(amidoamine) dendrimers-toward quantitative structure activity relationships. *Environ. Sci. Technol.* **43,** 6864–6869 (2009).

28. Suarez, I. J. *et al.* Chemical and ecotoxicological assessment of poly(amidoamine) dendrimers in the aquatic environment. *TrAC - Trends Anal. Chem.* **30,** 492–506 (2011).

29. Ulaszewska, M. *et al.* in *Analysis and Risk of Nanomaterials in Environmental and Food Samples, Comprehensive Analytical Chemistry* (ed. Damia Barcelo Marinella Farré) **59,** 197–233 (Elsevier, 2012).

30. Petit, A. N., Debenest, T., Eullaffroy, P. & Gagné, F. Effects of a cationic PAMAM dendrimer on photosynthesis and ROS production of Chlamydomonas reinhardtii. *Nanotoxicology* **6,** 315–326 (2012).

31. Gonzalo, S. *et al.* First evidences of PAMAM dendrimer internalization in microorganisms of environmental relevance: A linkage with toxicity and oxidative stress. *Nanotoxicology* **9,** 706–718 (2015).

32. Paerl, H. W. & Paul, V. J. Climate change: Links to global expansion of harmful cyanobacteria. *Water Res.* **46,** 1349–1363 (2012).

33. Rodea-Palomares, I. *et al.* Effect of PFOA/PFOS pre-exposure on the toxicity of the herbicides 2,4-D, Atrazine, Diuron and Paraquat to a model aquatic photosynthetic microorganism. *Chemosphere* **139,** 65–72 (2015).

34. Thompson, S. L., Manning, F. C. R. & McColl, S. M. Comparison of the toxicity of chromium III and chromium VI to cyanobacteria. *Bull. Environ. Contam. Toxicol.* **69,** 286–293 (2002).

35. Ando, T. *et al.* A novel method using cyanobacteria for ecotoxicity test of veterinary antimicrobial agents. *Environ. Toxicol. Chem.* **26,** 601–606 (2007).

36. Rodea-Palomares, I. *et al.* An insight into the

mechanisms of nanoceria toxicity in aquatic photosynthetic organisms. *Aquat. Toxicol.* **122–123,** 133–143 (2012).

37. Pandey, S., Rai, R. & Rai, L. C. Proteomics combines morphological, physiological and biochemical attributes to unravel the survival strategy of Anabaena sp. PCC7120 under arsenic stress. *J. Proteomics* **75,** 921–937 (2012).

38. Martín-Betancor, K. *et al.* Co, Zn and Ag-MOFs evaluation as biocidal materials towards photosynthetic organisms. *Sci. Total Environ.* **595,** 547–555 (2017).

39. Panda, B., Basu, B., Acharya, C., Rajaram, H. & Apte, S. K. Proteomic analysis reveals contrasting stress response to uranium in two nitrogen-fixing Anabaena strains, differentially tolerant to uranium. *Aquat. Toxicol.* **182,** 205–213 (2017).

40. Pulido-Reyes, G. *et al.* Physicochemical and biological interactions between cerium oxide nanoparticles and a 1,8-naphthalimide derivative. *J. Photochem. Photobiol. B Biol.* **172,** 61–69 (2017).

41. Gonzalo, S. *et al.* A Colloidal Singularity Reveals the Crucial Role of Colloidal Stability for Nanomaterials In-Vitro Toxicity Testing: nZVI-Microalgae Colloidal System as a Case Study. *PLoS One* **9,** e109645 (2014).

42. Shapiro, H. M. & Darzynkiewicz, Z. Practical Flow Cytometry (3rd edn). *Trends Cell Biol.* **5,** 372 (1995).

43. Elbaz, A., Wei, Y. Y., Meng, Q., Zheng, Q. & Yang, Z. M. Mercury-induced oxidative stress and impact on antioxidant enzymes in Chlamydomonas reinhardtii. *Ecotoxicology* **19,** 1285–1293 (2010).

44. Ahmed, S. Original Research Paper Biological Science Estimation of Total Chlorophyll and Total Carotenoid Contents for Strains of Anabaena and Gloeocapsa Through Spectrophotometer Part time Lecturer , Department of Botany , Dhing College , Dhing : Nagaon Assam KEYW. 70–71 (2016).

45. Lawrenz, E., Fedewa, E. J. & Richardson, T. L. Extraction protocols for the quantification of phycobilins in aqueous phytoplankton extracts. *J. Appl. Phycol.* **23,** 865–871 (2011).

46. Campbell, D. A., Hurry, V., Clarke, a K., Gustafsson, P. & Oquist, G. Chlorophyll fluorescence analysis of cyanobacterial photosynthesis and acclimation. *Microbiol. Mol. Biol. Rev.* **62,** 667–683 (1998).

47. Genty, B., Briantais, J. M. & Baker, N. R. The relationship between the quantum yield of photosynthetic electron transport and quenching of chlorophyll fluorescence. *Biochim. Biophys. Acta - Gen. Subj.* **990,** 87–92 (1989).

48. Pinto, F., Pacheco, C. C., Ferreira, D., Moradas-Ferreira, P. & Tamagnini, P. Selection of suitable reference genes for RT-qPCR analyses in cyanobacteria. *PLoS One* **7,** 1–9 (2012).

49. Van Kooten, O. & Snel, J. F. H. The use of chlorophyll fluorescence nomenclature in plant stress physiology. *Photosynth. Res.* **25,** 147–150 (1990).

50. Hartmut K, L. & Ursula, R. C R C Critical Reviews in Analytical Chemistry The Role of Chlorophyll Fluorescence in The Detection of Stress Conditions in Plants. *Crit. Rev. Anal. Chem.* **19,** 37–41 (1988).

51. Gonzalez-Pleiter, M. *et al.* Calcium mediates the cellular response of Chlamydomonas reinhardtii to the emerging aquatic pollutant Triclosan. *Aquat. Toxicol.* **186,** 50–66 (2017).

52. Livak, K. J. & Schmittgen, T. D. Analysis of relative gene expression data using real-time quantitative PCR and the 2-ΔΔCT method. *Methods* **25,** 402–408 (2001).

53. Prado, R., Rioboo, C., Herrero, C. & Cid, Á. Characterization of cell response in Chlamydomonas moewusii cultures exposed to the herbicide paraquat: Induction of chlorosis. *Aquat. Toxicol.* **102,** 10–17 (2011).

54. Torrecilla, I., Leganés, F., Bonilla, I. & Fernández-Piñas, F. Calcium transients in response to salinity and osmotic stress in the nitrogen-fixing cyanobacterium Anabaena sp. PCC7120, expressing cytosolic apoaequorin. *Plant, Cell Environ.* **24,** 641–648 (2001).

55. Barrán-Berdón, A. L., Rodea-Palomares, I., Leganés, F. & Fernández-Piñas, F. Free Ca2+ as an early intracellular biomarker of exposure of cyanobacteria to environmental pollution. *Anal. Bioanal. Chem.* **400,** 1015–1029 (2011).

56. K. Roháček. Chlorophyll fluorescence parameters the definitions photosynthetic meaning and mutual relationships. *Photosynthetica* **40,** 13–29 (2002).

57. Quenching, N. & Organisms, T. of I I. 1293–1298 (1996).

58. Mullineaux, C. W. & Allen, J. F. State 1-State 2 transitions in the cyanobacterium Synechococcus 6301 are controlled by the redox state of electron carriers between Photosystems I and II. *Photosynth. Res.* **23,** 297–311 (1990).

59. Kirilovsky, D. Photoprotection in cyanobacteria: the orange carotenoid protein (OCP)-related non-photochemical-quenching mechanism. *Photosynth. Res.* **93,** 7 (2007).

60. Latifi, A., Ruiz, M. & Zhang, C. C. Oxidative stress in cyanobacteria. *FEMS Microbiol. Rev.* **33,** 258–278 (2009).

61. Naha, P. C. Toxicology of Engineered Nanoparticles : Focus on Poly (amidoamine) Dendrimers. (2018). doi:10.3390/ijerph15020338

62. Kesharwani, P., Jain, K. & Jain, N. K. Dendrimer as nanocarrier for drug delivery. *Prog. Polym. Sci.* **39,** 268–307 (2014).

63. Svenson, S. & Tomalia, D. A. Dendrimers in biomedical applications-reflections on the field. *Adv. Drug Deliv. Rev.* **64,** 102–115 (2012).

64. Lesniak, W. G. *et al.* Biodistribution of Fluorescently Labeled PAMAM Dendrimers in Neonatal Rabbits: E ff ect of Neuroin fl ammation. (2013). doi:10.1021/mp400371r

65. Hong, S. *et al.* Interaction of polycationic polymers with supported lipid bilayers and cells: Nanoscale hole formation and enhanced membrane

permeability. *Bioconjug. Chem.* **17,** 728–734 (2006).

66. Singh, S. C., Sinha, R. P. & Hader, D. P. Role of lipids and fatty acids in stress tolerance in cyanobacteria. *Acta Protozool.* **41,** 297–308 (2002).

67. Imlay, J. A. Pathways of Oxidative Damage. *Annu. Rev. Microbiol.* **57,** 395–418 (2003).

68. Qian, H. *et al.* Effects of copper sulfate, hydrogen peroxide and N-phenyl-2-naphthylamine on oxidative stress and the expression of genes involved photosynthesis and microcystin disposition in Microcystis aeruginosa. *Aquat. Toxicol.* **99,** 405–412 (2010).

69. Prado, R., Rioboo, C., Herrero, C. & Cid, A. Screening acute cytotoxicity biomarkers using a microalga as test organism. *Ecotoxicol. Environ. Saf.* **86,** 219–226 (2012).

70. Naha, P. C. & Byrne, H. J. Generation of intracellular reactive oxygen species and genotoxicity effect to exposure of nanosized polyamidoamine (PAMAM) dendrimers in PLHC-1 cells in vitro. *Aquat. Toxicol.* **132–133,** 61–72 (2013).

71. Lazniewska, J. *et al.* Mechanism of Cationic Phosphorus Dendrimer Toxicity against Murine Neural Cell Lines. (2013). doi:10.1021/mp4003255

72. Geitner, N. K., Powell, R. R., Bruce, T., Ladner, D. A. & Ke, P. C. Effects of dendrimer oil dispersants on Dictyostelium discoideum. *RSC Adv.* **3,** 25930–25936 (2013).

73. Giraldez-Ruiz, N., Bonilla, I. & Fernadez-Piñas, F. The relationship between intracellular pH, growth characteristics and calcium in the cyanobacterium Anabaena sp. strain PCC7120 exposed to low pH. *New Phytol.* **137,** 599–605 (1999).

74. Geoffroy, L., Frankart, C. & Eullaffroy, P. Comparison of different physiological parameter responses in Lemna minor and Scenedesmus obliquus exposed to herbicide flumioxazin. *Environ. Pollut.* **131,** 233–241 (2004).

75. Misumi, M., Katoh, H., Tomo, T. & Sonoike, K. Relationship between photochemical quenching and non-photochemical quenching in six species of cyanobacteria reveals species difference in redox state and species commonality in energy dissipation. *Plant Cell Physiol.* **57,** 1510–1517 (2016).

76. Björkman, O. & Demmig, B. Photon yield of O2 evolution and chlorophyll fluorescence characteristics at 77 K among vascular plants of diverse origins. *Planta* **170,** 489–504 (1987).

77. Demmig-Adams, B., Garab, G., Adams III, W. & Govindjee, U. I. Non-photochemical quenching and energy dissipation in plants, algae and cyanobacteria. (2014).

78. Roháček, K. Chlorophyll fluorescence parameters: the definitions, photosynthetic meaning, and mutual relationships. *Photosynthetica* **40,** 13–29 (2002).

79. Franqueira, D., Orosa, M., Torres, E., Herrero, C. & Cid, Á. Potential use of flow cytometry in toxicity studies with microalgae Keywords. **247,** 119–126 (2000).

80. Albertazzi L., Serresi M., Albanese A., B. F. articles Dendrimer Internalization and Intracellular Trafficking in Living Cells. **57,** (2010).

81. Shukla, R. *et al.* HER2 Specific Tumor Targeting with Dendrimer Conjugated Anti-HER2 mAb. **17,** (2006).

82. Lee, I., Athey, B. D., Wetzel, A. W., Meixner, W. & Baker, J. R. Structural Molecular Dynamics Studies on Polyamidoamine Dendrimers for a Therapeutic Application: Effects of pH and Generation. 4510–4520 (2002). doi:10.1021/ma010354q

83. Leroueil, P. R. *et al.* Wide varieties of cationic nanoparticles induce defects in supported lipid bilayers. *Nano Lett.* **8,** 420–424 (2008).

84. Hong, S. *et al.* Interaction of poly(amidoamine) dendrimers with supported lipid bilayers and cells: Hole formation and the relation to transport. *Bioconjug. Chem.* **15,** 774–782 (2004).

85. Leroueil, P. R. *et al.* Nanoparticle interaction with biological membranes: Does nanotechnology present a janus face? *Acc. Chem. Res.* **40,** 335–342 (2007).

SUPPLEMENTARY INFORMATION

Mechanism of toxic action of cationic G5 and G7 PAMAM dendrimers in the cyanobacterium *Anabaena* sp. PCC 7120

Miguel Tamayo-Belda[a], Miguel González-Pleiter[a], Gerardo Pulido-Reyes[a], Keila Martin-Betancor[a], Francisco Leganés[a], Roberto Rosal[b], Francisca Fernández-Piñas[a,*]

Sergio Martínez-Campos[a], Miguel Redondo-Nieto[a], Juan Shang[c], Nuria Peña[c], Francisco Leganés[a], Roberto Rosal[b], Francisca Fernandez-Piñas[b,*]

[a] Department of Biology, Universidad Autónoma de Madrid, 28049 Madrid, Spain.
[b] Department of Chemical Engineering, Universidad de Alcalá, E-28871, Alcalá de Henares, Madrid, Spain.

* Corresponding author: francisca.pina@uam.es

Contents:

Table S2: Fluorochromes used to evaluate the physiological parameters by flow cytometry.

Fluorochrome	Acronym	Applications	Stock concentration (mg mL^{-1})	Final concentration (µg mL^{-1})	Incubation time (min)
2',7'-Dichlorofluorescin diacetate	H$_2$DCF DA	General level of Intracellular reactive oxygen species	1	100	30
Dihydrorhodamine123	DHR 123	Intracellular levels of hydrogen peroxide	2	10	40
Hydroethidine	HE	Intracellular levels of superoxide anion	3.154	5	30
Propidium iodide	IP	Membrane integrity	1	5	10
Fluorescein Diacetate	FDA	Non-specific esterase activity	5	2.5	15
bis-(1,3-dibutylbarbituric acid) trimethine oxonol	DiBAC$_4$(3)	Cytoplasmic membrane potential	0.5	2.5	10
CalciumGreen-1 acetoxymethyl ester	Calcium Green-1 AM	Intracellular free Ca^{2+}	2.6	8	120
20,70-bis(2-carboxyethyl)-5(6)-carboxy fluorescein	BCECF AM	Intracellular pH	1	5	40
OxyDNA Assay	OxyDNA Assay	Detection of 7,8-dihydro-8-oxo-2'-deoxyguanosine (8-OHdG), an important indicator of free radical-induced DNA damage and oxidative stress	1X	0.15X	30

Table S2: Effective concentrations of G5 and G7 dendrimers that induced 10%, 50% and 90% of growth inhibition over *Anabaena* growth after 72 h, expressed in mass concentration units, and the model type fitted.

Anabaena				
Compound	**Model fitted**	**EC$_{10}$** (mg/L)	**EC$_{50}$** (mg/L)	**EC$_{90}$** (mg/L)
G5	W1.2	1.27 ± 0.27	4.11 ± 0.30	8.68 ± 1.05
G7	W1.3	1.41 ± 0.29	9.07 ± 0.62	29.67 ± 2.47

.

Table S3: Experimental Degree of labeling (DOL), final Dendrimer:Alexa 488-conjugated concentration and related parameters.

PAMAM	MW (g/mol)	FG[1]	Initial concentration[2]		MR for optimal DOL[3]	Added dye[4] (μL)	Abs_{304} PAMAM:Alexa	Abs_{494} PAMAM:Alexa	Abs_{280} PAMAM at 1000 mg/L	Dilution Factor	Protein concentration (mg/L)
			(mg/L)	(μM)							
G5	28826	128	1000	34.69	19	2.9	0.02	0.10	0.21	20	880.19
G7	116493	512	1000	8.58	55	0.7	0.03	0.12	0.28	20	1220.07

1: Number of surface -NH$_2$

$$\frac{10 \times Abs_{494nm}}{71000 \times Dendrimer\ concentration\ (M)}$$

functional groups depending on the dendrimers generation.

2: Initial concentration (both in mg/L and mol/L) of the different PAMAM dendrimers used for the Alexa Fluor488 conjugation procedure.

$$\frac{10 \times [Abs_{280nm} - 0.11 Abs_{494nm}]}{\frac{Abs_{280nm\ of\ a\ dendrimer\ solution\ at\ 1\ mg/ml}}{molecular\ weight\ (Da)}}$$

3: Recommended amount in nanomoles of reactive dye that should be added for each nanomole of protein to be labeled, according to manufacturer instructions.

4: Added amount of Alexa Fluor 488 TFP ester dye to 1000 mg/L of PAMAM dendrimers according to the producer protocol)

5: Experimental DOL obtained for the different dendrimers. Experimental DOL was calculated as indicated by the producer's protocol:

DOL (mol dye/mol dendrimer) = ; where 71000 cm^{-1} M^{-1} is the approximate molar extinction coefficient of the Alexa

Fluor 488 dye. Dendrimer concentration (M) was calculated as indicated by the producer´s protocol adjusting the Abs_{280nm} (for detecting proteins) to Abs_{304nm}, where PAMAM dendrimers have their maximum absorption:

Where -0.11Abs_{494nm} is a correction factor for the contribution of the fluorophore to the absorbance at 280nm

6: Final concentration of Alexa Fluor488-conjugated PAMAM dendrimers: Dendrimer concentration (M)
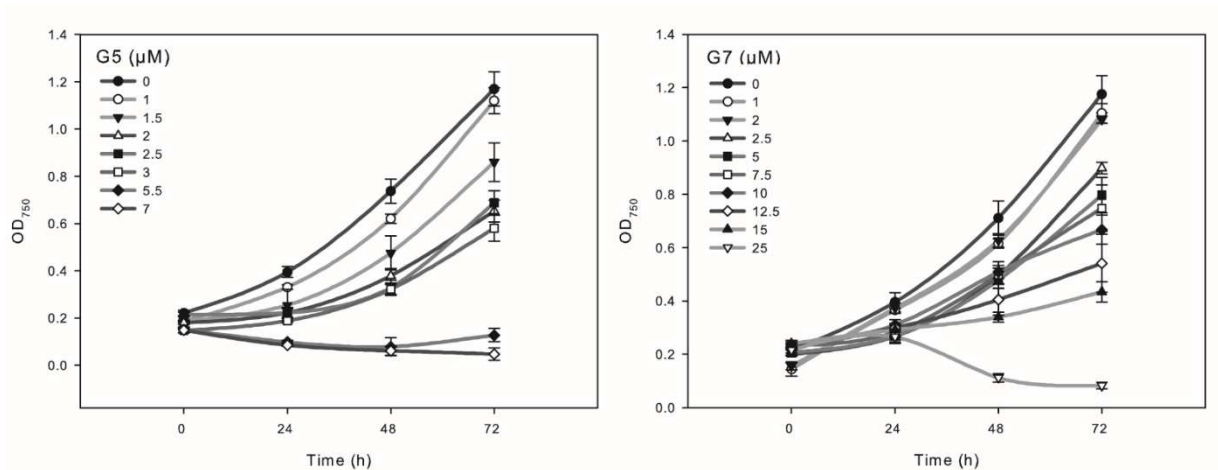
Figure S1: Dose-Response curves of *Anabaena* sp. PCC 7120 growth when exposed to increasing concentrations of G5 and G7 dendrimers.
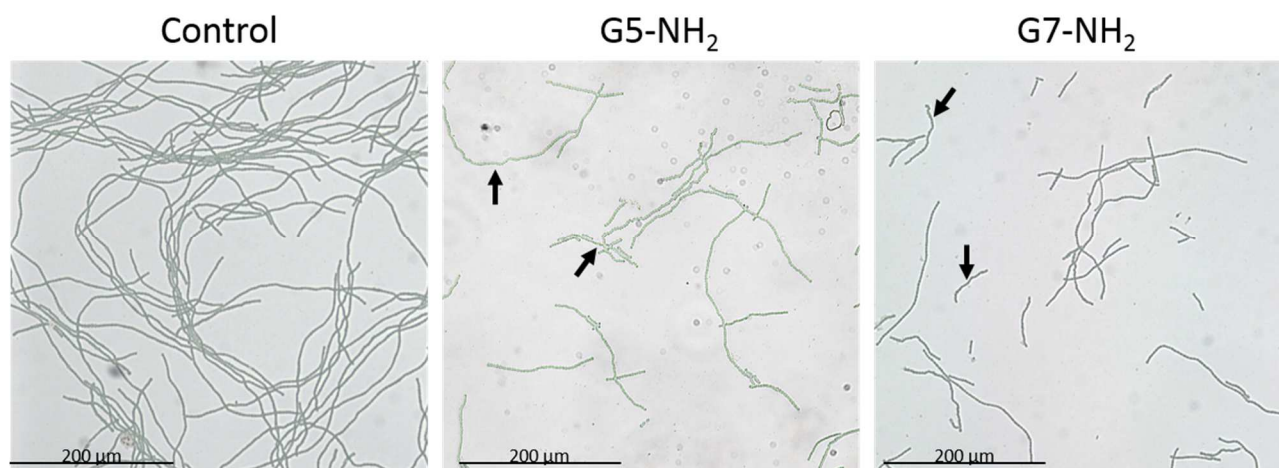

Figure S2: Optical images of *Anabaena* filaments. Black arrows indicate distorted filaments in the presence of dendrimers.
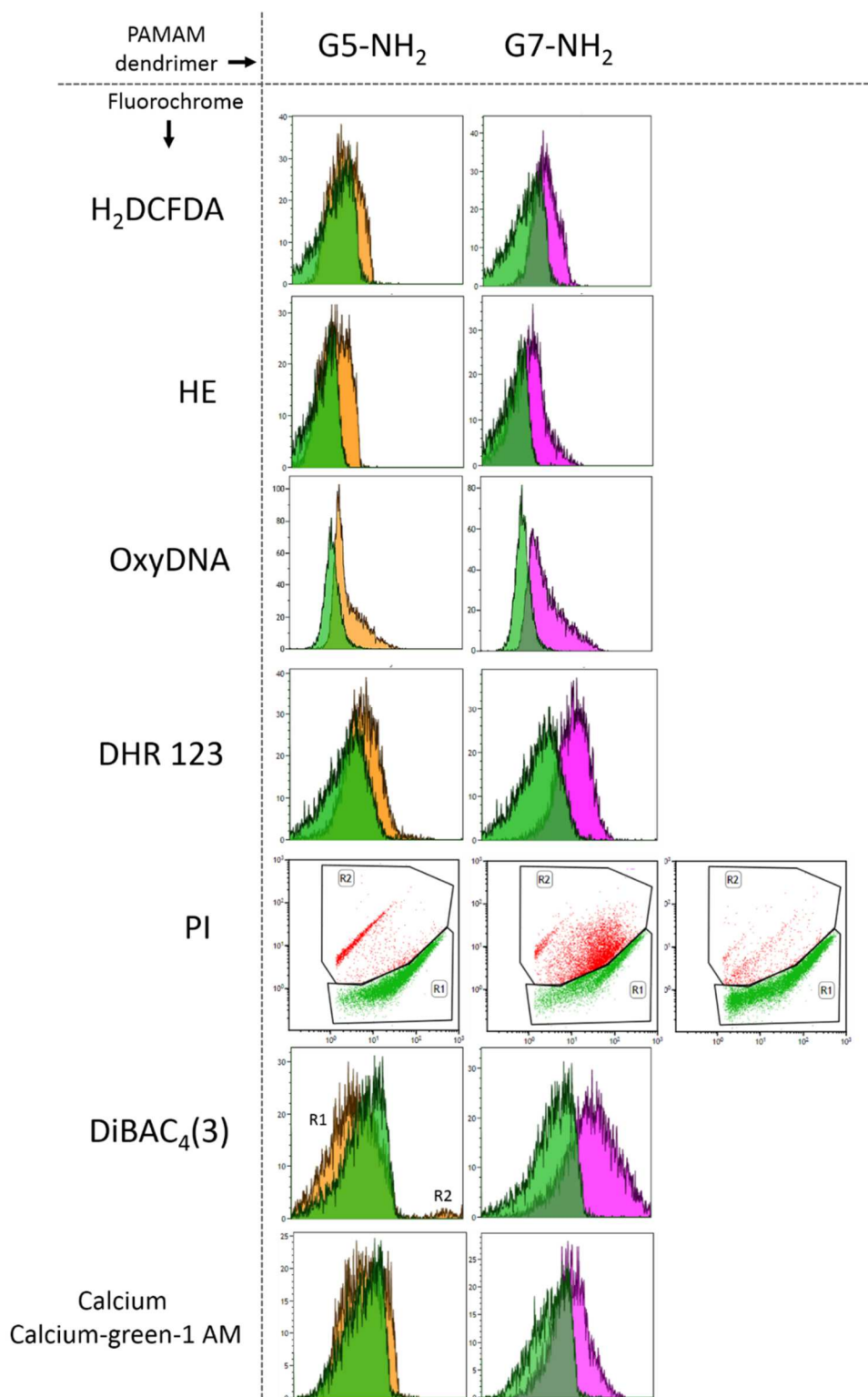
Figure S3: Flow cytometry results of the physiological parameters upon 72 h exposure of *Anabaena* sp. PCC 7120 to G5 and G7 PAMAM dendrimers. Representative result of the fluorochromes H_2DCFDA, DHR 123, HE, OxyDNA Assay, $DiBAC_4(3)$ and Calcium green-1 AM are shown through histograms (Y-axis: cell number, X-axis: fluorescence intensity in arbitrary units, a.u.); changes in the fluorescence intensity may be observed as shifts along the X-axis. PI results are shown as a dot plot (Y-axis: FL3, X-axis: FS) where: R1 (PI-; indicating the population of the cells which show normal membrane with no damage) and R2 (PI+; indicating the subpopulation of cells which show membrane damage). In all cases, green color represents the control.
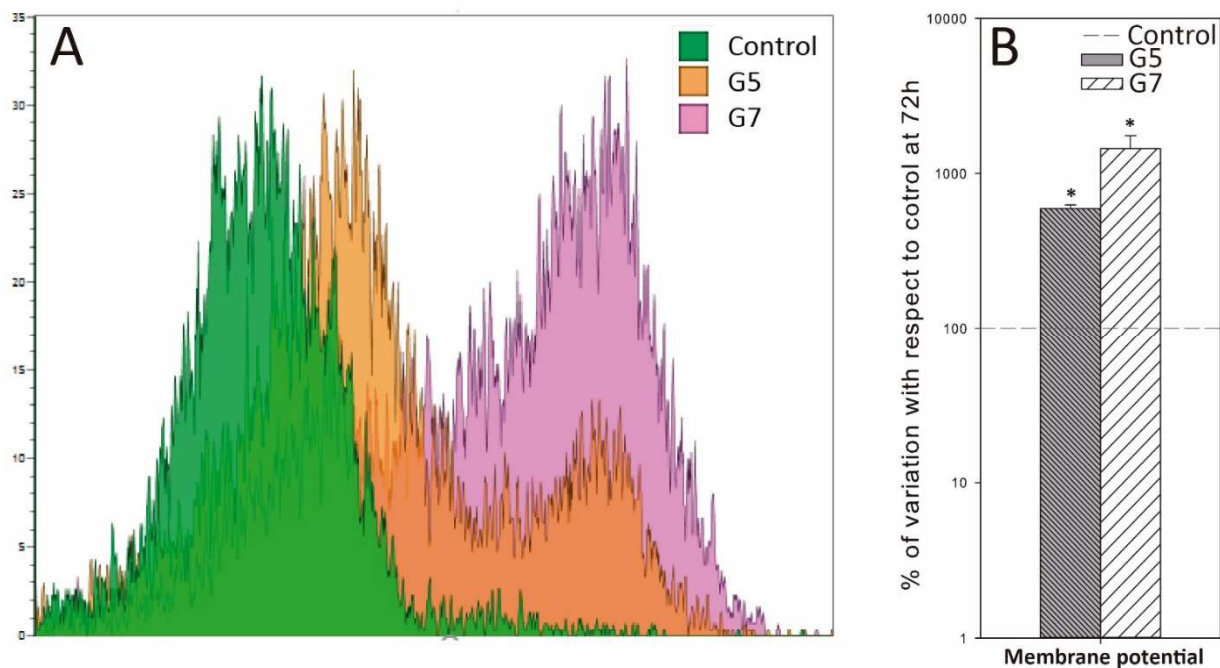
Figure S4: A: Representative flow cytometry histogram of the membrane potential measurement by using the fluorochrome $DiBAC_4(3)$ upon 72 h exposure of *Anabaena* sp. PCC 7120 to the concentration of G5 and G7 PAMAM dendrimers inducing 80% of growth inhibition (EC_{80}) (Y-axis: cell number, X-axis: fluorescence intensity in arbitrary units, a.u.); changes in the fluorescence intensity may be observed as shifts along the X-axis. B: Results represented as percentage of variation $\pm$ SD with respect to control (indicated as dashed line). Statistically significant differences ($p < 0.05$) are marked by asterisks (Tukey's HSD, $p < 0.05$).